

Shape of burning surface for solid propellant samples ignited with low laser heat flux

Quentin Levard *, Damien Noël *, Jouke Hijlkema*, Robin Devillers**, Nicolas Pelletier*

*ONERA/DMPE, Université de Toulouse, F-31410 Mauguac, France

**ONERA/DMPE, Université de Paris Saclay, F-91120 Palaiseau, France

Contact author: quentin.levard@onera.fr

Abstract

Unlike classical pyrotechnical solutions such as black powders, laser ignition is a non-intrusive, scalable method making it an interesting ignition technique for solid propellants in academia. When studies focus on the solid propellant gas flow, the shape of the burning surface becomes crucial. It is usually necessary to have a burning surface as flat as possible. The laser ignition delay of solid propellants follows a power law function of the laser heat flux. Because this law is not linear, ignition time varies strongly even for small laser irradiance variations. More precisely, the lower the laser irradiance, the more difficult it is to obtain a plane ignition. In this paper we present a calculation method to estimate the shape of the burning surface for a solid propellant sample based on the laser irradiance spatial distribution. For this purpose, a one-dimensional surface heating model is implemented together with a solid-propellant ignition model. This allows to calculate a local ignition delay as a function of the incident heat flux. The Gaussian spatial heat flux distribution has been discretised over the beam radius, and an ignition time calculation is performed for each spatial discretisation point. Considering that the solid propellant is a good thermal insulator, the ignition delay is independently calculated for each radius. Finally, the temporal evolution of the burning surface is determined, taking into account the flame propagation over the propellant surface. These results show the evolution of the surface with different laser parameters (i.e. beam size and power). This allows us to define, based on the laser irradiance distribution, a radius limit for which planar ignition can be assumed. An experimental setup is presented to measure the shape of the burning surface as a function of heat flux distribution for low laser irradiance. The calculation method is demonstrated with physical properties representative of a classical AP/HTPB research propellant composition. The approach is very promising to optimize ignition conditions for future experiments that require planar ignition.

Keywords: Laser ignition, Ignition model, Burning surface, Solid propellant

Nomenclature

A_p	Pre-exponential factor	$m \cdot s^{-1}$
α	Thermal diffusivity	$m^2 \cdot s^{-1}$
c_p	Heat capacity in the gas phase	$J \cdot kg^{-1} \cdot K^{-1}$
c_s	Heat capacity in the solid phase	$J \cdot kg^{-1} \cdot K^{-1}$
E_p	Activation energy in the solid phase	$J \cdot mol^{-1}$
e	Euler's number	(-)
k	Thermal conductivity	$W \cdot m^{-1} \cdot K^{-1}$
\dot{m}_p	Instantaneous propellant mass flow rate	$kg \cdot m^{-2} \cdot s^{-1}$
P_0	Laser power	W
Q_s	Heat released by surface reactions	$J \cdot K^{-1}$
q	Flux	$W \cdot m^{-2}$
R	Gas constant	$J \cdot mol^{-1} \cdot K^{-1}$
\dot{r}	Regression rate	$m \cdot s^{-1}$
T	Temperature	K
w	Laser beam radius (at $1/e^2$)	m
\cdot_p	Relative to propellant	(-)
λ	Wavelength	m
ρ	Density	$kg \cdot m^{-3}$

1. Introduction

Laser ignition is becoming more and more popular to study solid propellants and their behaviour thanks to its academic aspect [1] [2] [3] [4] [5]. As a matter of fact, laser ignition makes it possible to ignite solid propellants with an optical access (non-intrusive), without any foreign particles, and with a high precision level. For many experimental studies it is necessary to obtain an ignition surface shape as flat as possible, to control the evolution of the total burning surface for pressure prediction. It is important to notice that the ignition delay as a function of flux follows a power law. Therefore, the ignition front planarity is strongly dependent on the heat flux spatial distribution and the heat flux values [4]. That is why we designed a 1.5D code to calculate the radial propagation of solid propellant ignition over the sample surface, heated with a laser beam. In a first part, the problematic of low heat flux laser ignition will be presented, considering a Gaussian beam. Then a one-dimensional modelling of the heating of an inert material will be described, with the addition of an ignition criterion. Next a model will be proposed to calculate the ignition propagation along radius of a sample, depending on the laser ignition and the flame propagation. This modelling allows us to calculate the final shape of the burning surface of a solid propellant sample. Finally, an experimental setup is designed and used with the aim of studying the spatial evolution of the ignition propagation, and the spatial evolution of the extinction. Experimental results are presented and compared to the numerical calculations, highlighting an agreement between the experimental and numerical evolution of the ignition time as a function of the radius.

2. Problem description

2.1 Gaussian laser beam radius

The behaviour of a Gaussian laser beam depends on various parameters [4]. For a Gaussian beam propagating through space, the beam radius w will be minimal immediately at the exit of the laser, at the "waist". The radius w defines the transverse extension of the beam, i.e. its physical size perpendicular to the propagation direction. It is often defined by the beam radius at $1/e^2$, which is bounded by the points where the beam intensity reaches $1/e^2$ (about 13.5%) of its maximum value. The parameter w evolves linearly when we move far enough from the laser output. The angle between this straight line and the central axis of the beam is called the radial beam divergence θ .

The CO2 laser considered in this study has a wavelength of $\lambda = 10.6 \mu\text{m}$ and the diameter at the waist (at the laser output) is 3.6 mm, i.e., a radius $w_0 = 1.8 \text{ mm}$. As one moves away from the waist, the beam cross-section increases and the radius of curvature decreases until it passes through a minimum in a section at a distance $z_0 = \pi w_0^2 / \lambda$, called the Rayleigh distance. At the distance z_0 from the waist, the cross-section has doubled from the minimum cross-section and the beam radius is such that:

$$w(z = z_0) = w_0 \sqrt{2} \quad (1)$$

Moving away from the waist, the laser beam seems to be contained within an envelope but in reality, the beam does not have a well-defined contour. It is therefore necessary to specify the criterion used in the definition of the radius or diameter. At $1/e^2$, the radius in the section z is equal to:

$$w(z < z_0) = w_0 \left(1 + \left(\frac{\lambda z}{\pi w_0^2} \right)^2 \right)^{\frac{1}{2}} = w_0 \left(1 + \left(\frac{z}{z_0} \right)^2 \right)^{\frac{1}{2}} \quad (2)$$

We speak of near field or Rayleigh region on a distance z_0 . Beyond this distance, the beam is contained within a cone of angle at the top given by the divergence. Therefore, the radius in the section z is given by:

$$w(z > z_0) = z\theta \quad (3)$$

The Figure 1 shows the evolution of the beam radius $w(z)$ as a function of the propagation distance, from the analytical expressions presented above. The transition at z_0 is abrupt but the values are in good agreement with the values given in the documentation of the laser used in this study.

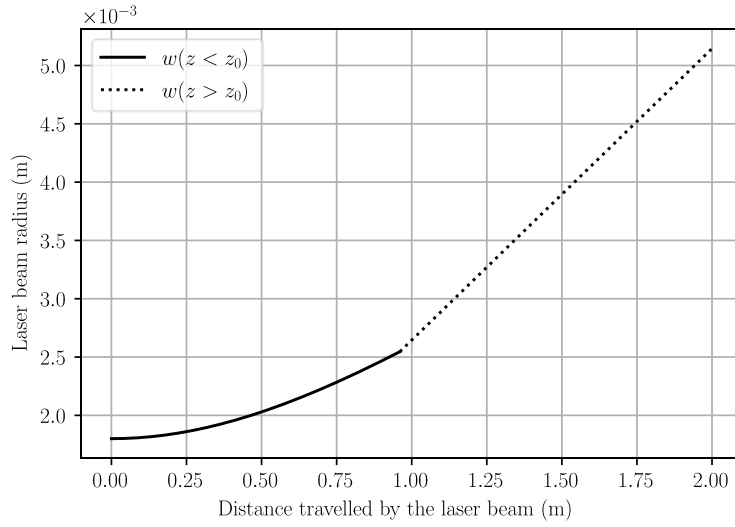


Figure 1 : Laser beam radius at $1/e^2$ as a function of the distance travelled by the laser beam

2.2 Gaussian heat flux distribution

The heat flux spatial distribution of a Gaussian laser beam, also named irradiance, remains constant during the laser beam propagation. The flux density profiles are axisymmetric and decrease as the distance from the centre of the beam increases perpendicular to the propagation direction. Thus, in a section of radius $w(z)$ at the distance z from the waist, the laser flux $q(r = 0, z)$ on the axis of a beam ($r = 0$) carrying a power P_0 , is given by:

$$q(r = 0, z) = q_0(z) = \frac{2P_0}{\pi w(z)^2} \quad (4)$$

The flux at any point (r, z) of the section z is given by:

$$q(r, z) = q_0(z) \exp\left(-\frac{2r^2}{w(z)^2}\right) = \frac{2P_0}{\pi w(z)^2} \exp\left(-\frac{2r^2}{w(z)^2}\right) \quad (5)$$

Assuming that the laser power is contained entirely within a section of diameter $2w$, the mean flux in the beam is $q_{mean}(z) = P_0/(\pi w(z)^2)$. This allows to obtain the Figure 2, with the Gaussian and the mean distribution of the flux for determined laser power, laser beam radius and distance z from the laser source.

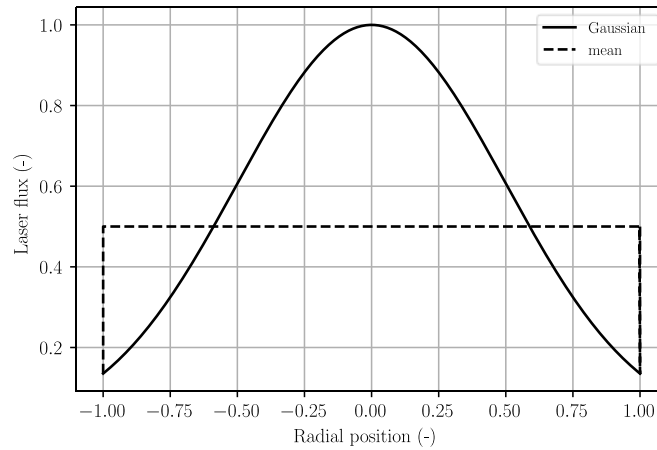


Figure 2 : Normalized Gaussian and mean distribution of the laser flux for given laser power P_0 , laser beam radius w and distance z from the laser source

It is possible to adjust the laser flux either by modifying the laser power carried by the laser beam for a fixed radius or by modifying the laser beam radius at constant laser power. Adjusting these parameters induces variations of the local laser heat flux at the surface of the solid propellant sample.

2.3 Non-linearity of the ignition time as a function of the flux

The literature presents numerous studies on the dependence between ignition delay and flux. This has been investigated in particular in the context of laser ignition [6]. The ignition time t_{ign} as a function of the laser flux q follows a power law such as:

$$t_{ign} = A_0 q^{B_0} \quad (6)$$

where A_0 and B_0 are real numbers. For opaque materials, $B_0 \sim -2$ [6].

The difference of ignition time is significantly more important at low flux, because of the power law. As a consequence, when using a low-powered laser, some issues may be encountered at low flux if the flux deposited is not properly mastered, as the Figure 3 shows. Neighbouring spots of a solid-propellant sample might ignite with a significant time difference when low laser-power levels are used.

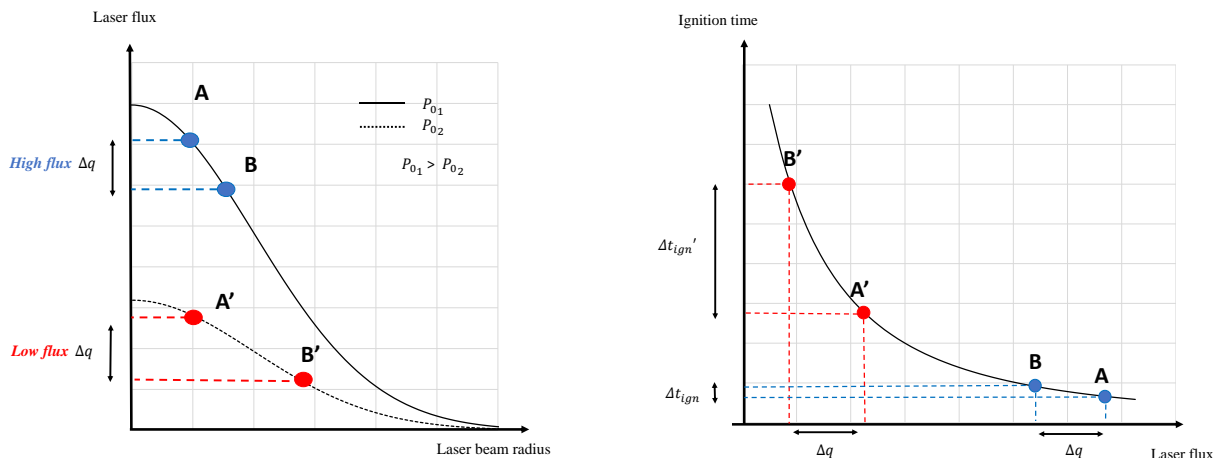


Figure 3 : Gaussian spatial distribution of the flux (left) and ignition time vs. laser flux (right)
[For the same Δq , $\Delta t_{ign}' \gg \Delta t_{ign}$ because of the power law ruling ignition as a function of the laser flux]

For a Gaussian distribution and a low power laser, moving from the centre the laser flux drops slightly. Therefore, the ignition time increases significantly which leads to a non-planar surface. This motivates the present study in order to optimize sample ignition for low laser-power levels.

3. One-dimensional ignition model

3.1 Heating of an insulating pyrolyzable material

Thermal model

In order to determine the ignition time and ignition temperature of solid propellants, a one-dimensional model based on the unsteady heating of the propellant by conduction on its surface and its surface decomposition at regression rate \dot{r} is used. In our case, a constant laser flux is heating the propellant surface. Thus, a simplified model with superficial heating is considered. The heat flux applied at the propellant surface and the energy release or consumption due to phase transition reactions and pyrolysis of the solid phase are supposed to be concentrated at the surface. This consideration is justified by the high insulating power of solid propellants [7].

For a material with non-temperature dependent thermophysical properties, the equation to be solved in a frame of reference related to the combustion surface is:

$$\frac{\partial T(z, t)}{\partial t} + \dot{r}(t) \frac{\partial T(z, t)}{\partial z} = \alpha \frac{\partial^2 T(z, t)}{\partial z^2} \quad (7)$$

Mass conservation in the solid phase (assuming a single component system) states that the rate of change of the mass within the solid phase is due to the regression of the solid propellant surface, multiplied by the density:

$$\dot{m}_p(t) = \rho_p \dot{r}(t) \quad (8)$$

At the solid propellant surface, the regression rate \dot{r} is defined by:

$$\dot{r}(t) = \begin{cases} A_p \exp\left(-\frac{E_p}{R T_s(t)}\right) & \text{if } T_s(t) < T_{s,ign} \text{ (pyrolysis)} \\ ap^n & \text{else (combustion)} \end{cases} \quad (9)$$

with:

- $T_s(t) = T(0, t)$: surface temperature of the solid propellant (K)
- a : Vieille's law coefficient (–)
- p : pressure (Pa)
- n : pressure exponent of Vieille's law (–)

It leads to the following pyrolysis flux, at the propellant surface:

$$q_{pyrolysis}(t) = \dot{m}_p(t) Q_s = \rho_p A_p \exp\left(-\frac{E_p}{R T_s(t)}\right) Q_s \quad (10)$$

The flux provided by the flame written q_{flame} is also considered, using a simplified superficial model which does not describes precisely the flame contribution. It is estimated by performing an energy balance between the flame and the solid propellant surface and remains constant.

Initial conditions

At $t = 0$, the solid propellant surface is at ambient temperature and the constant laser flux noted as q_{laser} is null.

$$\begin{cases} \forall z \in]-\infty, 0], & T(z, 0) = T_0 \\ & q_{laser}(0) = 0 \end{cases} \quad (11)$$

Boundary conditions

To evaluate the heat flux penetrating at the solid propellant surface, a surface absorption model is used considering an opaque material which is a strong assumption for AP/HTPB solid propellants [3]. An empirical parameter is introduced and allows a smooth transition from a heating model to a stationary combustion regime. The transition from one to another is progressive. The boundary condition 2 (BC2) describes the thermal balance between the solid phase and the gaseous phase inspired by [7]. Consequently, boundary conditions are:

$$\begin{cases} \mathbf{BC1} : T(-\infty, 0) = T_0 \\ \mathbf{BC2} : -k \frac{\partial T(z, t)}{\partial z} \Big|_{z=0} = q_{laser} - q_{pyrolysis}(t) + (1 - \beta) q_{flame} \end{cases} \quad (12)$$

with:

- T_0 : ambient temperature (K)
- $q_{pyrolysis}$: flux consumed by the pyrolysis ($W \cdot m^{-2}$)
- q_{flame} : flux provided by the flame ($W \cdot m^{-2}$)
- β : transition parameter to transit from heating to combustion

Numerical scheme

The finite difference approach is used to solve the system of equations. An appropriate robust scheme is required, because throughout the transient ignition regime, the problem can quickly change from a diffusion-dominated to a convection-dominated situation, leading to significant stability problems. A time-explicit and space-centered scheme is used. The heat equation at the next time step becomes [8]:

$$T_j^{n+1} = T_j^n + \frac{\alpha \Delta t}{\Delta z^2} (T_{j+1}^n - 2T_j^n + T_{j-1}^n) - \frac{\dot{r} \Delta t}{2\Delta z} (T_{j+1}^n - T_{j-1}^n) \quad (13)$$

with:

Δt : time step (s)

Δz : space step (m)

α : thermal diffusivity of solid propellant ($m^2 \cdot s^{-1}$)

T_j^n : temperature of the propellant in slice j at time n (K)

Using appropriate boundary conditions as we have done, the temperature profile inside the solid propellant can be established by iterating forward in time from the initial temperature distribution T_0 until an ignition criterion is reached. The time and space step must be carefully set in order to avoid stability problems. To do so, the CFL condition must be respected and is given by:

$$\Delta t \leq \frac{\Delta z^2}{2\alpha} \quad (14)$$

$$\Delta z \leq \frac{\alpha}{2\dot{r}} \quad (15)$$

Ignition criterion

There are many theories regarding the determination of an ignition criterion for a propellant and there are also many different methods for determining whether propellant ignition has occurred, both in experimental and numerical studies. From a theoretical perspective, ignition is generally defined as having occurred when a certain surface temperature has been reached [9].

In this study, ignition ($T_s(t_{ign})$) is detected when the surface temperature deviates significantly from that of an inert material [9]. This observation makes it possible to determine the dependencies between the ignition surface temperature and the incident laser flux. This temperature $T_{s,ign}$ is used to determine the ignition instant, i.e. the time where $T_s(t) = T_{s,ign}$.

3.2 Results

Surface temperature heating process

When the propellant sample is subjected to a constant laser heat flux, its surface temperature evolves in two distinct phases: first, a material heating phase which results in a relatively slow progression of the surface temperature, then an ignition phase following an acceleration of the pyrolysis reactions which results in a very sharp increase in temperature (Figure 4).

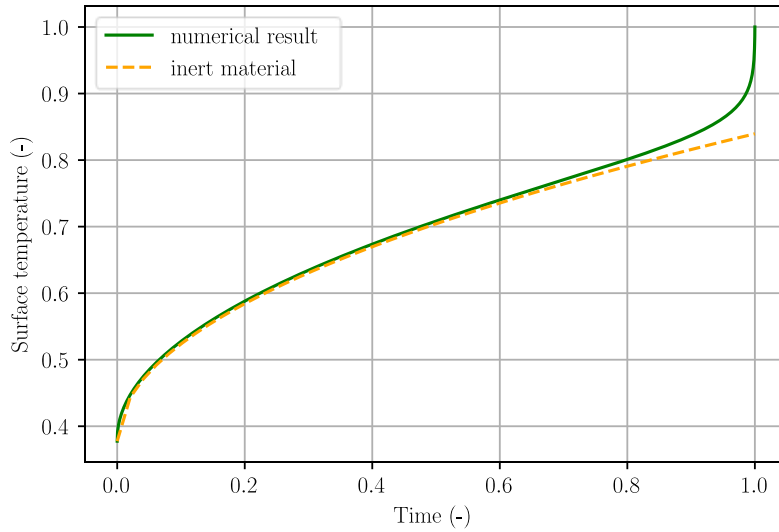


Figure 4 : Normalized Surface temperature vs. Time for a solid propellant and an inert material heated by a constant laser flux

During the inert heating phase, the surface temperature evolution is governed by the heat flux received and the thermal properties of the material, in this case the thermal effusivity $E = (k_p \rho_p c_s)^{1/2}$ if its properties are independent of temperature or, in the more general case, of thermal conductivity, density and mass heat capacity. When considering the heating of an inert material, the thermal profile in the material is given by [9] :

$$T(z, t) = T_0 + \frac{2q_{laser}}{k_p} (\alpha t)^{\frac{1}{2}} \operatorname{ierfc} \left(\frac{z}{2(\alpha t)^{\frac{1}{2}}} \right) \quad (16)$$

Which gives for a surface temperature deduced for $z = 0$:

$$T_s(t) = T_0 + \frac{2q_{laser}}{k_p} \left(\frac{\alpha t}{\pi} \right)^{\frac{1}{2}} = T_0 + \frac{2}{\pi^{\frac{1}{2}}} \frac{q_{laser}}{E} t^{\frac{1}{2}} \quad (17)$$

This expression clearly presents the dependence of the surface temperature on the value of the flux q_{laser} and on the physical properties through the thermal effusivity. For a given propellant, $T_s(t^{1/2})$ has a slope proportional to q_{laser} , which is very useful to effectively determine the laser flux deposited on a sample from an experimental point of view when the material properties are assumed to be independent of temperature as in our case.

4. Ignition modelling of a solid propellant surface irradiated with a Gaussian laser beam

4.1 Method

In order to model the ignition of a propellant surface heated by a Gaussian laser beam, the 1D model for solving the heat equation is used in conjunction with the Gaussian laser beam model. The spatial distribution of the flux being Gaussian, it evolves with the distance from the centre of the laser beam. By discretizing the Gaussian distribution into several elements on which the laser flux will be considered constant, it is possible to approximate the ignition time of each discretised element as a function of the distance from the centre of the laser beam.

To focus on the ignition time in the plane (radius, ignition time) as a function of the Gaussian distribution of the flux, the Gaussian distribution is discretized over the $1/e^2$ radius of the laser beam, as shown in the Figure 5 with 30 elements.

The elements are delimited by the blue nodes and the red vertical lines. The black points correspond to the laser flux values at the centre of each element. By increasing the discretization, the accuracy is improved. The final model is used with 200 elements over the diameter of the laser beam.

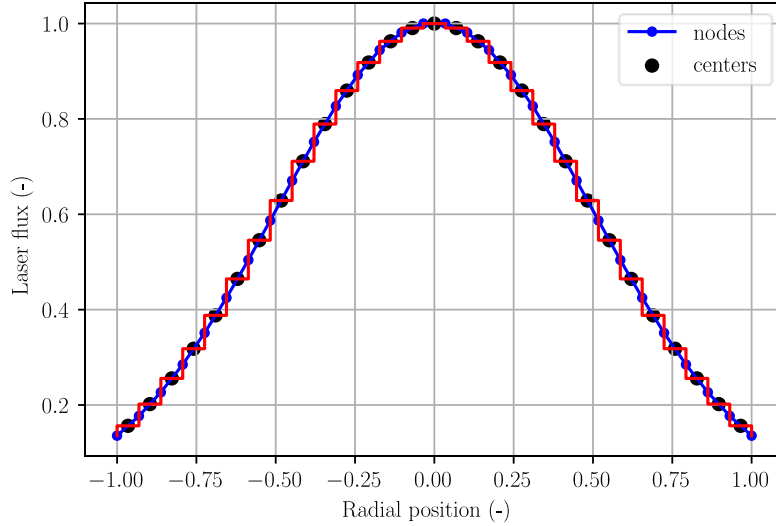


Figure 5 : Spatial discretisation of the laser flux distribution for given laser power P_0 and laser beam radius at $1/e^2$ w

4.2 Laser ignition velocity vs. Flame propagation velocity

For a given solid-propellant sample, two phenomena generate ignition: a) direct ignition by the laser heat flux, b) lateral flame propagation, i.e. ignition induced by a neighbouring portion that is already ignited. For this model we consider the competition between the autonomous flame propagation v_{flame} and the propagation of the laser ignition v_{laser} . The laser ignition propagation is defined as:

$$v_{laser} = \frac{\delta r}{\delta t_{ign}} \quad (18)$$

with: $\delta r = r_i - r_{i-1}$: difference between the radial position of two adjacent cells
 $\delta t_{ign} = t_{ign}(r_i) - t_{ign}(r_{i-1})$: difference between the ignition time of two adjacent cells

The one-dimensional code is used to calculate the ignition time of each elementary cell (Figure 6). For small radii, close to the centre of the laser beam, the level of flux causes a laser ignition propagation v_{laser} larger than the flame spreading velocity v_{flame} (autonomous propagation of the flame over the solid propellant surface). The ignition time is therefore governed by the laser ignition time calculated (Figure 6) and named $t_{ign,laser}$. Then, the decrease in flux (due to the Gaussian distribution of the flux) implies a very significant increase of the ignition time [4] (Figure 6) and consequently a lower laser ignition propagation. When the laser ignition propagation becomes lower than the flame velocity, then the ignition delay becomes flame-driven. By determining the coordinates $(r_{transition}, t_{transition})$ of the point where this transition occurs, we can determine the shape of the ignition, with a part related to the ignition by the laser flux and a linear part related to the ignition by the flame (Figure 7). This is summarised by:

$$t_{ign} = \begin{cases} t_{ign,laser} & \text{if } v_{laser} > v_{flame} \\ t_{ign,flame} & \text{else} \end{cases} \quad (19)$$

with: $t_{ign,flame} = (r - r_{transition})/v_{flame}$ where r is the distance from the center of the laser beam.

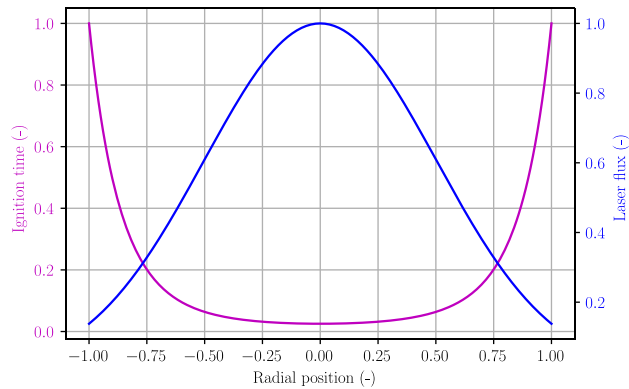


Figure 6 : Normalized ignition time and laser flux vs. laser beam radius in each discretised element for a given laser beam radius at $1/e^2$ and a laser power P_0

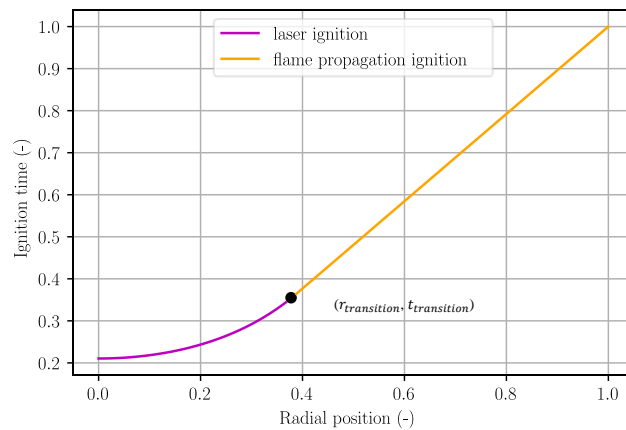


Figure 7 : Normalized Ignition time vs. Distance from the centre of the laser beam for given laser power P_0 , laser beam radius w , flame velocity v_{flame}

4.3 Shape of burning surface

From the ignition delay curve as a function of radius for a given set of parameters (P_0, w, V_f), it is possible to obtain the geometric shape of the laser ignition by considering a regression of the propellant by parallel layers at constant velocity v_{reg} . The approach used here is purely geometrical. The first observation is that the first point lighting up in the centre of the beam forms a zero angle with the horizontal and regresses vertically. This is the starting point of the calculation. From then on, the geometrical shape of the ignition is reconstructed until the ignition reaches the edge of the propellant surface, noted A (Figure 8), where the flux is minimal.

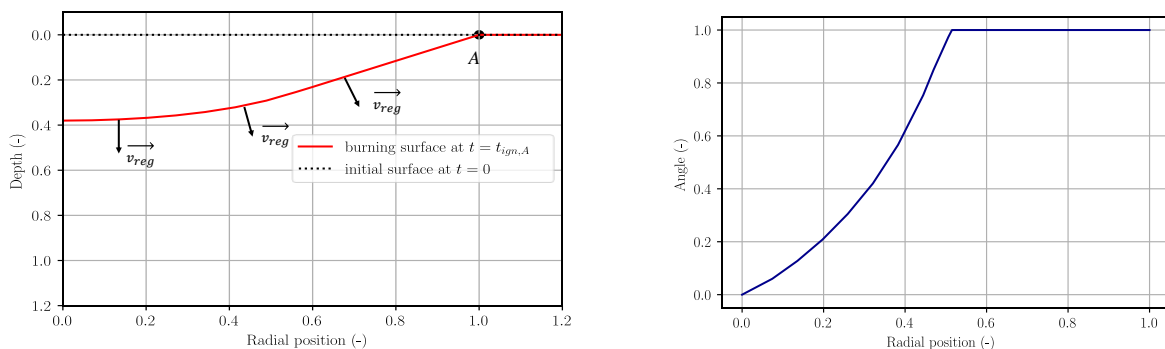


Figure 8 : Normalized burning surface regression for given laser power ($P_0, w, v_{flame}, v_{reg}$) at ignition of point A (left) and associated angle to the horizontal (right)

With the geometrical evolution of the combustion angle, it is then possible to impose a condition of flatness with an angle criterion (Figure 8). Considering that the maximum tolerable angle to the horizontal is 15° , we obtain the radius for which the regressing surface can no longer be considered as flat. This delimitation of the "plane" ignition radius, which depends on the flux and therefore on the power and the radius of the laser beam, is represented by the vertical dotted asymptotes in the Figure 9.

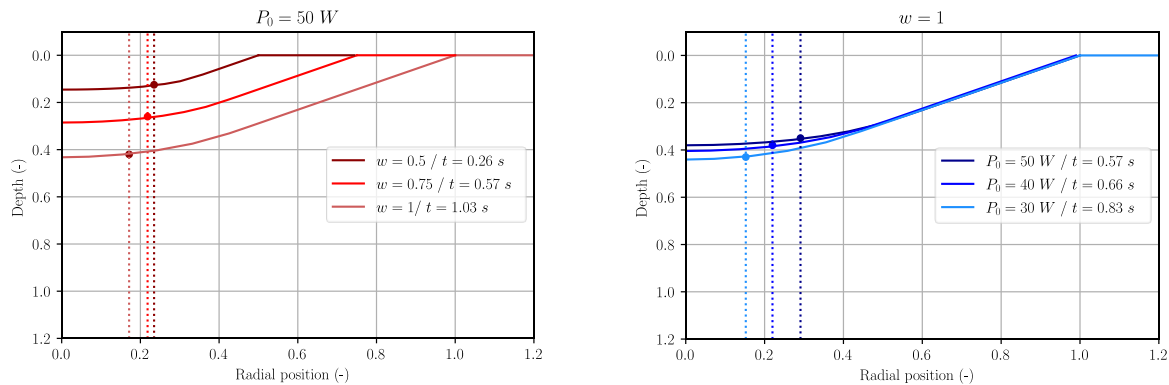


Figure 9 : Normalized burning surface regression for given flame velocity v_{flame} and regression velocity v_{reg} . Parametrical studies have been performed on the influence of laser power P_0 (right) and laser beam radius w (left) on the «planar radius »

5 Experimental study

5.1 Experimental setup

To validate the 1.5D numerical code presented in section 4, an experimental set-up was designed to allow the ignition of a solid propellant sample and the measurement of the ignition time radial evolution. The laser used for this study is a 50W CO₂ laser source. The numerical study allowed us to highlight a point of interest in terms of spatial flux distribution for beam radii about 5 mm diameter at 50W power. The use of a beam expander and the distance between the laser source and the sample allows to reach a theoretical beam radius of 5 mm at $1/e^2$. Mirrors are used to deflect the beam and permit vertical ignition. The assembly was self-collimated to minimise alignment errors. The sample is placed on a PMMA plate and is observed with two high-speed cameras: the first one targets the ignition propagation on the top side of the sample (with a 45° angle vision), whereas the second camera targets portions of the sample where the full height has burned and flame is visible with a view from below, through the PMMA plate (Figure 10). The extinction visualisation allows observation of the trace left by the ignition (laser, pyrotechnic ignitor, hot wire, ...) in the sample without harsh ignition conditions [10].

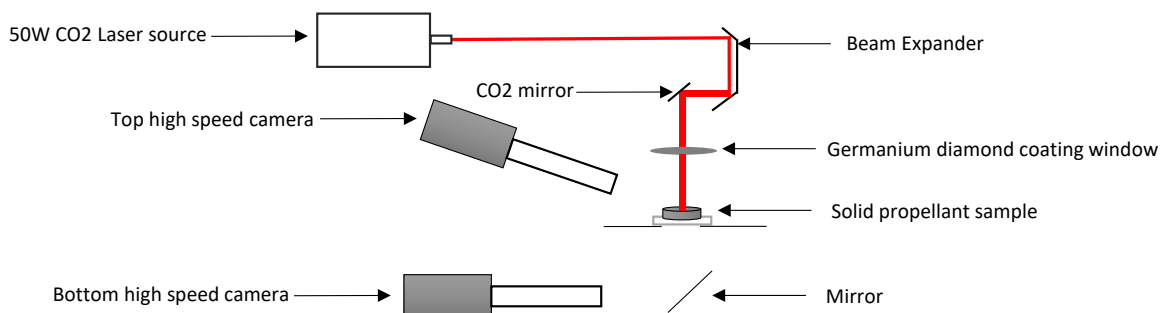


Figure 10 : Diagram of the experimental set-up

5.2 Results

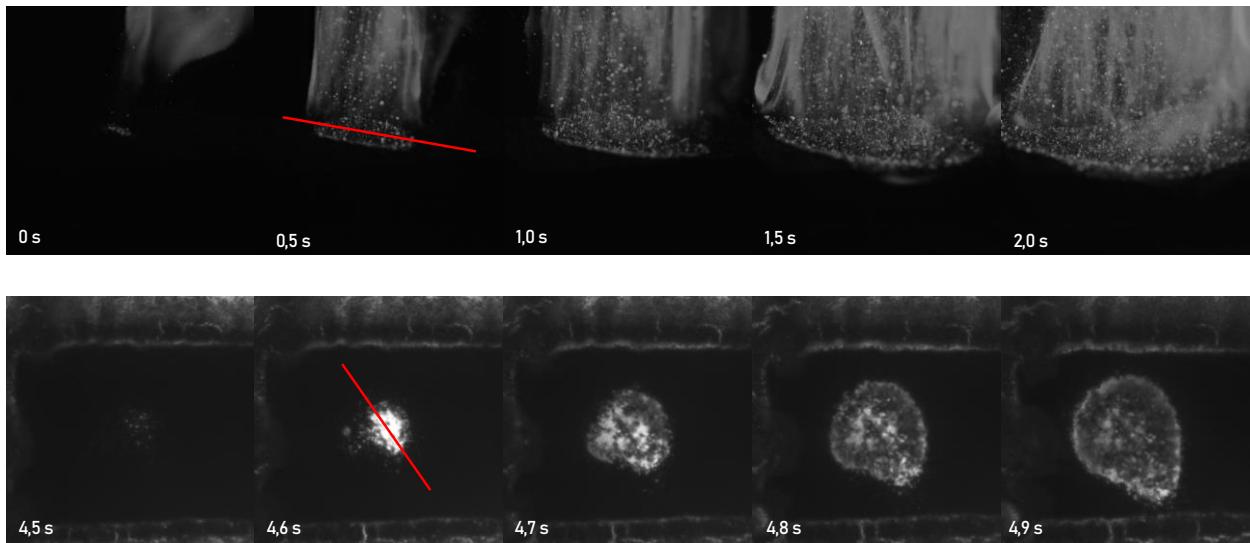


Figure 11 : Visualisation of ignition (top) and extinction (bottom) of the solid propellant sample with time

We can see on Figure 11 the evolution of the ignition front and the extinction front over time. The time reference $t = 0s$ is fixed when the first flame light appears. We can notice that the time scale is different for ignition and extinction views, because the discovery of the sample is faster due to the geometry evolution during regression. We can notice with the bottom view that extinction (and therefore ignition) isn't circular but elliptical, with a coma's shape (Figure 16) and a radius ratio of about 1.2 between the major axis and the minor axis. It will therefore be interesting to pay particular attention to the spatial distribution of the experimental laser beam (Figure 15). The delay of 4s corresponds to the time to consume the sample thickness in the middle.

After signal thresholding, the evolution of the number of white pixels is plotted over time to measure the evolution of the luminosity along a line. The line is positioned along the longest axis of the ellipse in order to measure of common data between the two visualisations. The data is then spatially scaled using a test pattern to plot the radius of the ignition and the extinction delay as a function of the radius. Figure 12 shows the ignition and extinction curves of the same test (ignition test 3 and extinction test 3), and a second ignition curve as a comparison. The extinction curve of the second test is missing due to a camera trigger fault. First, we observe a very good reproducibility of the ignition. When comparing the measurements at ignition and extinction, the same shape is observed. We can also notice a scale effect on the radius, corresponding to a change of transition radius ($r_{transition}$ in Figure 7) due to the propagation of the combustion angle (projection of the angle with the dotted line). The extinction measurement can be used as a validation of the ignition measurement because it is spatially better defined, because of the angle propagation, i.e. the measurement has more spatial resolution (pixel size) with the same optical setup. The laser source is turned off at 0.5s and it is noticeable that the combustion is already autonomous at this time. Therefore, the laser shut off has no influence on the ignition geometry. It can also be observed that the shape of the extinction front is identical to the ignition front (no variation in slope between 0 and 2 mm), so it can be concluded that there is no acceleration of combustion due to the laser. The laser flux becomes negligible in relation to the flame when we consider only the flame propagation.

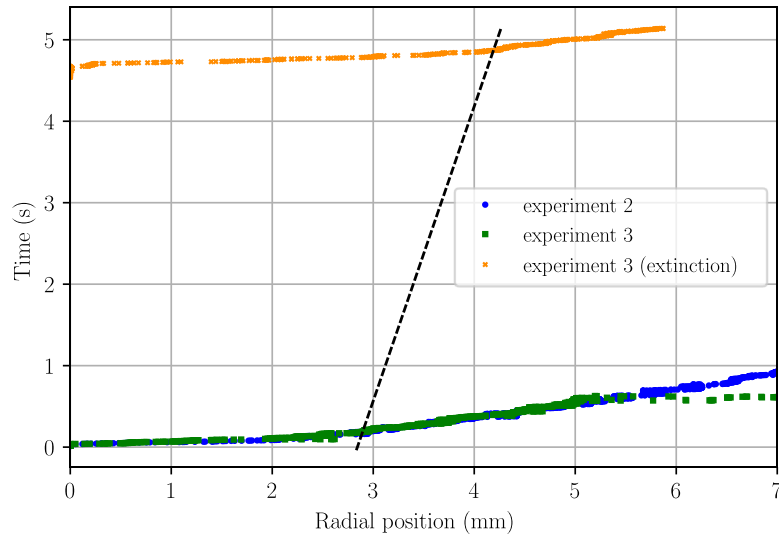


Figure 12 : Measurement of the ignition time and the extinction time as a function of the radial position

5.3 Comparison with the numerical calculus

Experimental and numerical results were compared in order to analyse the validity of the modelling approach. Numerical calculations were performed on an AP/HTPB composite propellant. The thermal properties summarize in Table 1 allow an estimation of the thermal diffusivity.

Table 1 : Thermal properties of the solid propellant composition [7]

		Value
k_p	Thermal conductivity ($W \cdot m^{-1} \cdot K^{-1}$)	~ 0.4
ρ_p	Density ($kg \cdot m^{-3}$)	~ 1700
c_s	Heat capacity in the solid phase ($J \cdot kg^{-1} \cdot K^{-1}$)	~ 1100

The flame spreading velocity was measured at $v_{flame} = 5.65$ mm/s and the regression velocity at $v_{reg} = 1.3$ mm/s. The total power received by the propellant sample was calculated using an inertial fluxmeter. Assuming that the laser power distribution is perfectly Gaussian over a laser beam radius of $w = 4.5$ mm, the measured flux corresponds to a laser power P_0 . These parameters are given in Table 2.

Table 2 : Parameters used in numerical calculation

		Value
w	Laser beam radius (mm)	4.5
v_{flame}	Flame spreading velocity ($mm \cdot s^{-1}$)	5.65
v_{reg}	Regression velocity ($mm \cdot s^{-1}$)	1.3

All the following numerical results are calculated with data given in Table 1 and Table 2.

Shape of burning surface for solid propellant samples ignited with low laser heat flux

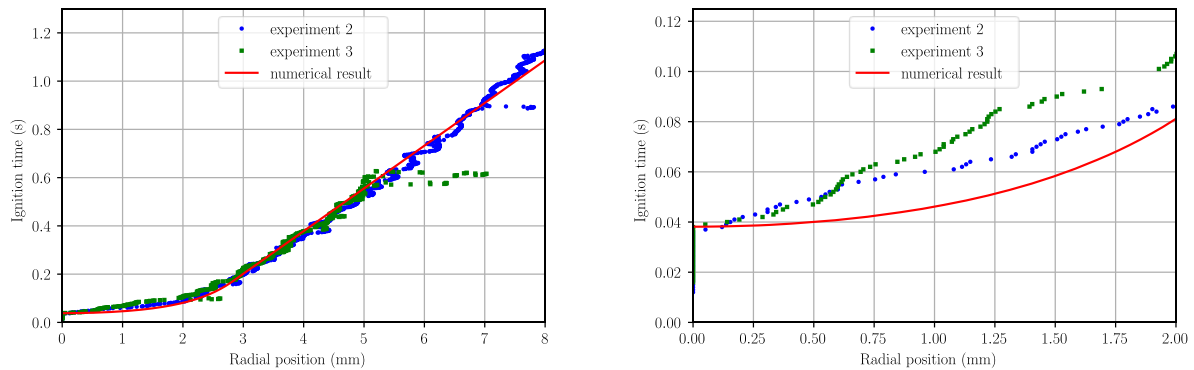


Figure 13 : Numerical and experimental comparison of ignition delay versus radius (right: zoom on 0 – 2 mm radius)

The Figure 13 presents the comparison between the test results and the calculation performed with the above data. The curves seem to be in good agreement. The two behaviours, laser-driven and flame-driven ignition, described in the numerical part, can be observed. The autonomous flame speed is exactly the same as the experiment, which is not surprising since the experimental value is used as input for the numerical estimation. However, the slope of the laser ignition and the determination of the inflection point between the laser ignition and the flame propagation are both well reproduced. The modelling presented in the part 4.2 is therefore representative of the experiments, and captures the transition radius. Finally, the 1.5D code can be used as a robust first approach in order to determine the ignition delay as a function of the radius, for a laser ignition. However, a specific look (Figure 13 right) at the laser ignition phase underscores that experimental ignition time is constantly higher for low radii.

Consequently, it is possible to project the ignition delay of each point of the surface to calculate the shape of the solid propellant sample, and finally verify the ignition planarity. As an example, Figure 14 gives the shape of the burning surface calculated at different times from the numerical curve plotted in Figure 13. The maximum angle to the horizontal is only dependent on the flame propagation and regression velocity. In this case it does not exceed 15° .

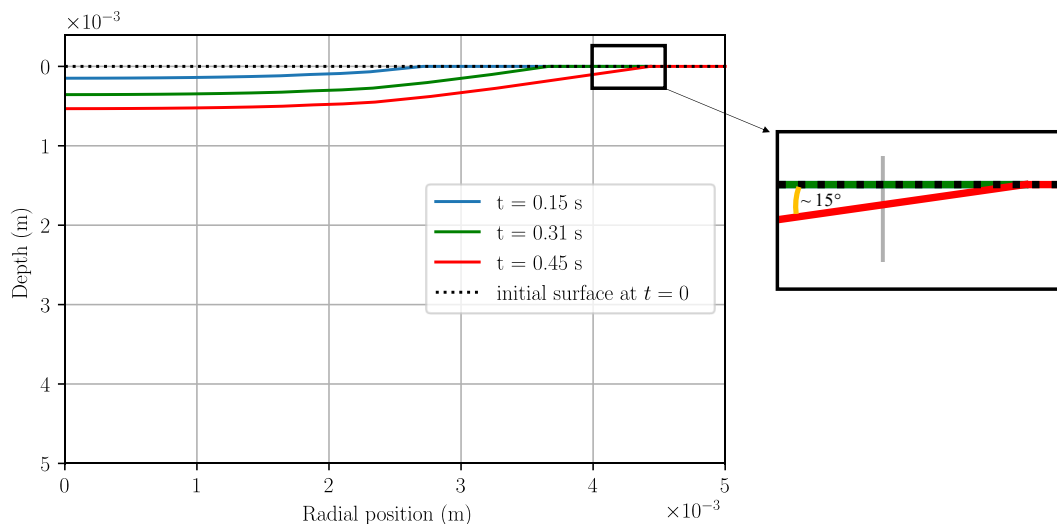


Figure 14 : Rebuilding of burning surface regression from the numerical result corresponding to the experiment

We noticed that the experimental ignition time is systematically higher for lower radii than those predicted by the model. A possible explanation would be that the hypothesis of a pure Gaussian distribution is not valid. To verify this, we hit a PMMA sample with a 15 second laser pulse (PMMA absorbs the CO₂ laser radiation completely). Figure 15 shows the trace of the laser impact compared to a Gaussian distribution. We see that the trace looks more like an arrow

than a Gaussian. This could explain the deficit of heat flux for low radii, and hence the underestimation of the ignition propagation for these points. The vertical view of the trace (Figure 16) shows the coma's shape of the spatial distribution. This could be due to a misalignment of the mirrors in the laser cavity leading to a coma aberration.

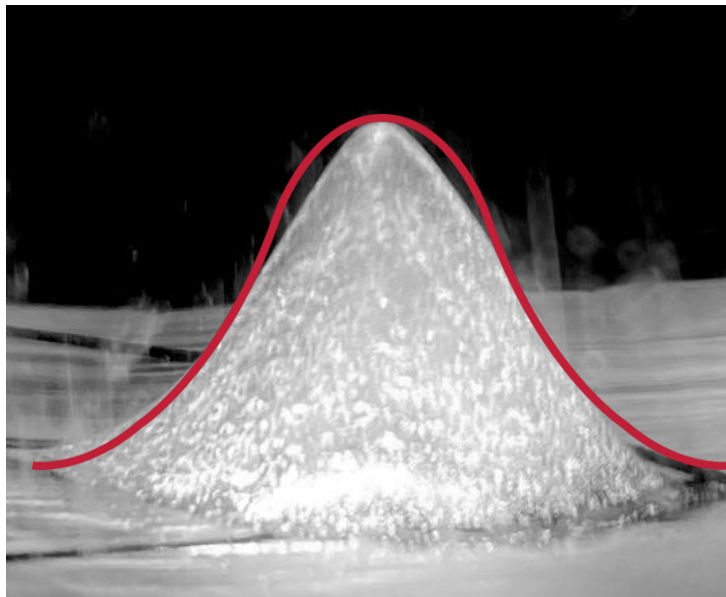


Figure 15 : Trace deposited by the laser beam in PMMA compared to a Gaussian distribution



Figure 16 : Vertical view of the trace deposited by the laser beam in PMMA

6 Conclusion

Shape and quality of a solid propellant laser ignition are not equivalent in case of high heat flux condition or in low heat flux condition. Indeed, because of the power shape of the ignition time as a function of the heat flux, the ignition geometry of a solid propellant sample depends on the spatial distribution of the laser beam power, but it also depends on the heat flux value. More accurately, a high flux ignition will be more planar than low flux ignition. It is therefore interesting to study the geometry induced by laser ignition for low power laser sources. A 1D calculation code was produced to calculate the ignition time as a function of the laser incident flux. The spatial heat flux distribution of the laser has been discretised over the Gaussian laser beam radius, and an ignition time calculation is performed for each spatial discretisation point. Then a model has been proposed to represent the transition from the laser ignition phase to the flame propagation phase. This transition modelling permits to calculate the ignition propagation over the complete sample surface. The ignition time as a function of the radius can be used to calculate the ignition front propagation and thus calculate the sample geometry during the combustion. To assess this model, an experimental set-up has been designed. A solid propellant sample is heated with a CO₂ laser beam and observed with 2 high speed cameras. The first camera visualises the top side of the sample, measuring the spatial distribution of the ignition time, whereas the second camera visualises the spatial distribution of the sample extinction. The comparison of these two measurements is consistent and highlights no regression acceleration due to the laser beam. These results underline that the combustion of the solid propellant follows a parallel layer regression. Finally, a calculation of the evolution of the ignition time with the radius is made to be compared with the experimental results. This calculation reproduces very

closely the shape of the experimental ignition delay curve and confirms the quality of the model. It allows to clearly distinguish the two ignition regimes (laser ignition then autonomous flame propagation) but especially reproduce the same transition radius. An effort could still be made to better reproduce the spatial distribution of the experimental flux to try to be even more accurate.

References

- [1] C. Zanotti and P. Giuliani, "Composite propellant ignition and extinction by CO₂ laser at subatmospheric pressure," *Propellants, Explosives, Pyrotechnics*, pp. 254-259, 1998.
- [2] A. I. Atwood, K. P. Ford, D. T. Bui, P. O. Curran and T. Lyle, "Radiant ignition studies of ammonium perchlorate based propellants," *Progress in propulsion physics*, pp. 121-140, 2009.
- [3] J. Cain and M. Q. Brewster, "Radiative Ignition of Fine-Ammonium Perchlorate Composite Propellants," *Propellants, Explosives, Pyrotechnics: An International Journal Dealing with Scientific and Technological Aspects of Energetic Materials*, vol. 31, no. 4, pp. 278-284, 2006.
- [4] J. J. Granier, T. Mullen and M. L. Pantoya, "Nonuniform laser ignition in energetic materials," *Combustion Science and technology*, pp. 1929-1951, 2003.
- [5] A. D. Baer and N. W. Ryan, "Ignition of composite propellants by low radiant fluxes," *AIAA journal*, vol. 5, no. 3, pp. 884-889, 1965.
- [6] L. Strakovskiy, A. Cohen, R. Fifer, R. Beyer and B. Forch, "Laser Ignition of Propellants and Explosives," *ARL-TR-1699*, 1998.
- [7] O. Orlandi, J. Dupays and F. Fourmeaux, "Ignition Study at Small-Scale Solid Rocket Motor," in *EUCASS 2019*, Madrid, 2019.
- [8] A. Harrland and I. A. Johnston, "Review of Solid Propellant Ignition Models Relative to the Interior Ballistic Modelling of Gun Systems," *DSTO-TR-2735*, 2012.
- [9] G. Lengellé, A. Bizot, J. Duterque and J. C. Amiot, *Allumage des propergols solides*, La Recherche Aérospatiale, 1991.
- [10] J. Hijlkema and Q. Levard, "On the optical verification of the influence of the ignition on the regression surface of a cigarette-burning small-scale solid rocket motor," in *Space Propulsion*, Estoril, 2022.